Experimental evaluation of diamond burnishing for sustainable manufacturing

To cite this article before publication: Sachin B *et al* 2018 *Mater. Res. Express* in press https://doi.org/10.1088/2053-1591/aadb0a

Experimental evaluation of diamond burnishing for sustainable manufacturing

Sachin B[a]*, Narendranath S[a], D Chakradhar[b]

[a]Department of Mechanical Engineering, National Institute of Technology Karnataka, Surathkal, India

[b]Indian Institute of Technology Palakkad, Kerala, India

*Corresponding author email: sachinraobc@gmail.com

Abstract: Diamond burnishing is one of the most popular surface finishing technique used to achieve an excellent surface finish. The aim of the present study is to investigate the effect of process parameters in diamond burnishing of 17-4 PH stainless steel (PH SS) under cryogenic environment. The requirement of a sustainable environment for various machining processes urged to explore the importance of cryogenic burnishing over other cooling techniques. Surface modification was achieved by the application of liquid nitrogen (LN_2) during diamond burnishing. The process parameters considered to reduce the surface roughness (Ra) and increase the surface hardness (H) are burnishing speed, burnishing feed and burnishing force. The diamond burnishing experiments were conducted based on the L_9 orthogonal array. The significant parameters and the optimal level of each parameters were determined by using analysis of variance (ANOVA) and main effect plots respectively. Multi-response optimization has been carried out for cryogenic diamond burnishing of 17-4 PH stainless steel by using Taguchi's grey relation analysis (TGRA). From the TGRA, it was observed that at burnishing speed 73 m/min, burnishing feed 0.048 mm/rev and burnishing force 150 N, improved diamond burnishing performance characteristics were obtained. An improvement in grey relation grade (GRG) was found to be 38.47%. Cryogenic diamond burnishing has led to modifications in the microstructure and also an improvement in the subsurface hardness of the material.

Keywords: Diamond burnishing, 17-4 PH stainless steel, surface roughness, microhardness.

1. Introduction

17-4 PH stainless steel has high toughness, high impact and tensile strength properties thus it can be classified under difficult to cut materials [1]. Some of the important applications of 17-4 PH stainless steel are steam turbines, chemical industry, marine construction and power plants [2]. Surface treatment techniques are one of the finest methods to improve the surface topography of the material by subjecting it to severe plastic deformation. Many secondary manufacturing techniques produce irregularities, voids, flakes etc. However to avoid these problems, chipless finishing process such as burnishing is widely used in modern applications. An accurate surface profile of the specimen can be achieved by diamond burnishing process with a little plastic deformation. Redistribution of the grains on the surface layer takes place without any material loss. Irregularities of the surface are pressed down and distended up because of the burnishing process which leads to an excellent surface finish. In the present investigation, diamond burnishing tool is used in order to get the enhanced surface integrity properties. Diamond tip can be used for the inner and outer circumferential surfaces of workpiece [3]. The working principle of the diamond burnishing process is based on an indenting diamond tool which moves along the cylindrical length of the workpiece. Due to the force acting on the workpiece by the diamond tip, the plastic flow of the asperities occurs and will be flattened. The major applications of the diamond burnishing process are crankshafts, valves, railway, spacecraft, defense, aircraft, machine tools etc. [4]. Yu and Wang [5] studied the effect of polycrystalline diamond tool on surface roughness of aluminium alloy. It was observed that the surface roughness of a burnished aluminium alloy has been decreased from 0.5µm to 0.026µm. It was reported by Nestler and Schubert [6] that the surface roughness can be reduced along with the reduction in the voids formation. It was found that the burnishing feed is the parameter which has more influence on surface roughness. The mass of the component can be reduced and performance will be improved by using slide diamond burnishing process in AA2124.

The high temperatures generated while finishing process can be reduced with the application of a variety of coolants. Conventional coolants have been utilized by metal cutting industries to reduce the machining zone temperatures. It is not preferable to use conventional coolants because of its influence on some of the factors such as environmental aspects, health and production cost etc. [7]. Cryogenic burnishing is one of the most environmentally friendly

processes, wherein it could avoid health problems, chip cleaning cost and maintenance cost etc. In the present work LN_2 is considered as the coolant which has been maintained at a temperature of −196 °C and it will be sprayed to the tool-workpiece interface. The temperature at the interface will be reduced because of the constant supply of the liquid nitrogen at the interface. Yang et al. [8] have studied the effect of severe plastic deformation process and cryogenic burnishing on the modifications of surface integrity of Co-Cr-Mo alloy. It was observed that the temperature induced can be significantly removed by the application of LN_2. Microstructural modifications and improved hardness have been observed after cryogenic burnishing. Caudill et al. [9] compared the effect of cryogenic, flood-cooled and dry burnishing on surface integrity of Ti-6Al-4V alloy by severe plastic deformation technique. It was revealed that in the severe plastic deformation, layer which was produced by cryogenic environment showed improved grain structure, increased hardness, and improved surface finish.

Quality and productivity are the two major factors which have to be considered as most important in manufacturing industries. To obtain a good quality products effective selection of process parameters are very much necessary. One of the scientific techniques which have been effectively used to solve multi-objective optimization problems is TGRA. Aggarwal et al. [10] obtained optimal process parameters of machining under cryogenic environment by using desirability function analysis. An improvement in the GRG has been noticed by Tang et al. [11] while optimizing the process parameters of EDM by using TGRA. Chakradhar and Gopal [12] optimized the process parameters of electrochemical machining (ECM) of EN 31 steel by using TGRA. It was noticed that feed rate is the most significant parameter which affects the ECM robustness. Sivaiah and Chakradhar [13] carried out multi-objective optimization of cryogenic turning process on 17-4 PH stainless steel by using GRA. It was concluded that feed rate is the most significant parameter on turning performance characteristics. Sivaiah and Chakradhar [14] optimized the process parameters of turning by using TGRA. The feed rate was proved to be the most influencing parameter on performance characteristics of turning with a percentage of contribution of 53.76.

From the literature about the diamond burnishing process, it has been observed that only a few researchers concentrated on the optimization of process parameters of diamond burnishing process under different lubricating media. 17-4 PH stainless steel is one of the widely used material

in manufacturing industries, because of its excellent strength and corrosion resistance properties. Hence it is important to carry out the optimization studies of diamond burnishing process to enhance the surface integrity properties of the material. The present study focuses on the analysis of the diamond burnishing process parameters namely burnishing speed, burnishing feed and burnishing force on 17-4 PH SS under cryogenic environment. An optimum cutting condition is found from the burnishing responses such as surface roughness and surface hardness using TGRA. Microstructure, microhardness and surface topography were analyzed under cryogenic environment.

2. Experimental details

Diamond burnishing experiments were performed on 17-4 PH stainless steel cylindrical bars of diameter 32 mm and length of 150 mm. The experimental information is as shown in Table 1. Cryogenic burnishing setup and burnishing zone are shown in Figure 1 and Figure 2 respectively. In order to fix one side of the cylindrical workpiece in the chuck, facing operation has been performed and center drill operation has been carried out on both the ends of the workpiece. The top layer of the workpiece has been removed with the help of tungsten carbide insert and the diameter will be reduced to 30 mm for the diamond burnishing operation. Alcohol was used to clean the surface of the workpiece before burnishing operation. This will remove the foreign particles which will be accumulated in the gap between the tool and the workpiece interface. Based on the preliminary tests the diamond burnishing process parameters were determined and the range of the levels were selected by considering the possible minimum, medium and maximum values.

Table 1. Experimental information

Workpiece material and dimensions	17-4 PH stainless steel round bar, (⌀ 30 mm x 150 mm)
Chemical composition	(Ni-3.546 %, Cr-16.179 %, Cu-3.177 %, Mn-0.744 %, Si-0.360 %, C-0.042 %, P-0.028 %, S-0.011 %, Nb+Ta-0.356 % and Fe-Balance)
Tool used	Diamond burnishing tool (DB200)
Coolant used	Liquid nitrogen (LN_2)
Burnishing fluid supply	Cryogenic cooling - compressed air: 4 kg/cm^2, flow rate: 0.45 kg/min (through external nozzle)
Nozzle diameter	1 mm

Table 2. Factors and levels

Code	Control factor	Level		
		1	2	3
A	Burnishing speed (m/min)	21	73	113
B	Burnishing feed (mm/rev)	0.048	0.065	0.096
C	Burnishing force (N)	20	90	150

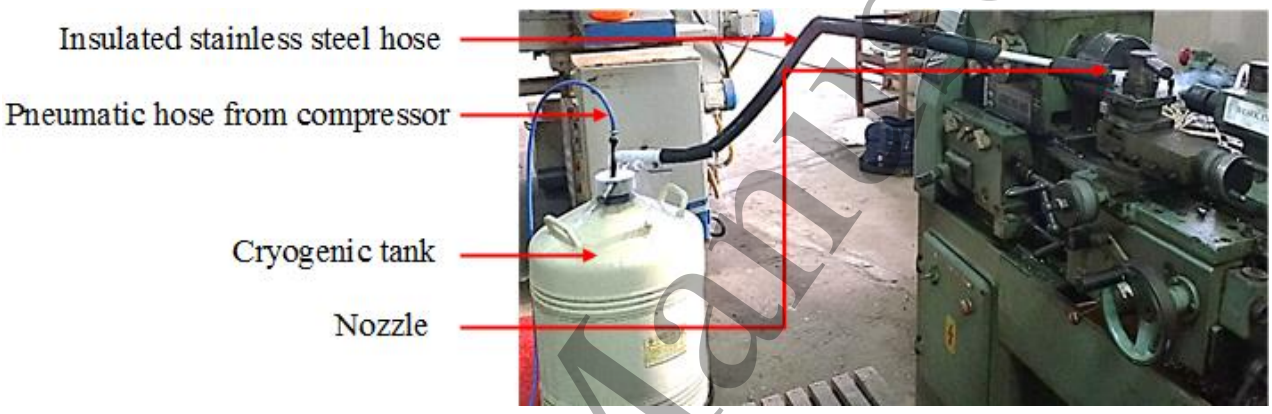

Figure 1. Cryogenic diamond burnishing setup

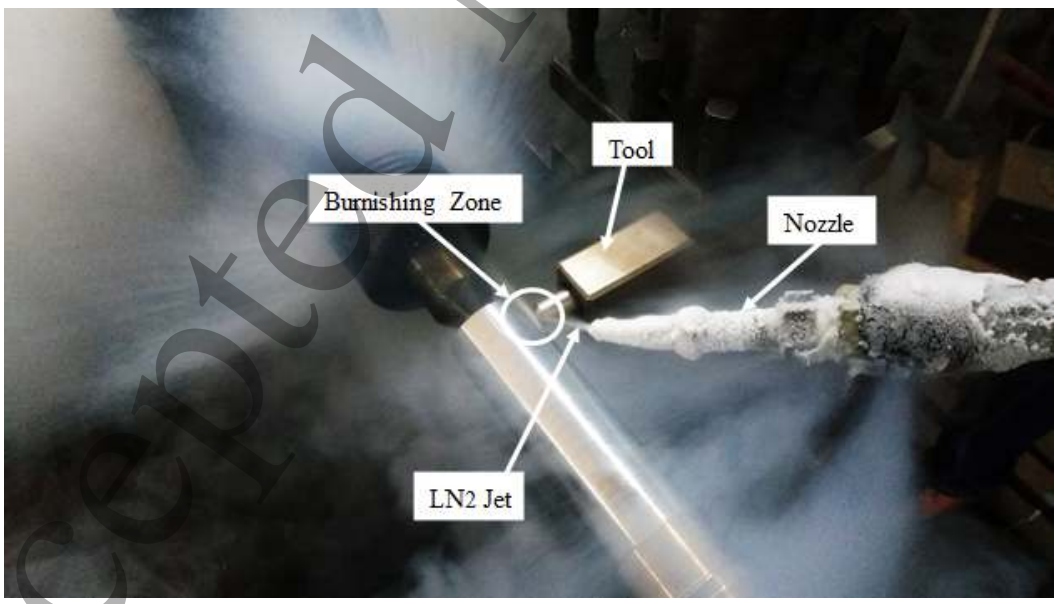

Figure 2. Burnishing zone of cryogenic burnishing experiments

In the present investigation, three process parameters namely burnishing speed, burnishing feed and burnishing force were selected and tested under cryogenic environments. The process parameters and their levels are as depicted in Table 2. Nine experiments were performed based on an L_9 orthogonal array. The obtained experimental results of surface roughness and surface hardness are tabulated in Table 3. The surface roughness of the workpiece was measured by using SJ301 'Mitutoyo' surface roughness tester. The surface hardness was measured by using Vickers hardness tester 'VM-120'. The samples were cold mounted, polished with different grades such as 600, 800, 1000, 1500, 2000 grit emery papers to obtain the mirror finish and cleaned with ethanol. Optical microscope (BIOVIS material plus) was used to observe the microstructural changes. Subsurface microhardness of the specimen was measured using OMNI TECHMVHS-AUTO-type Vickers microhardness tester. Five different areas were selected to measure the surface roughness and surface hardness values. The average of five readings was taken as the final value of the responses. The average values of surface roughness and hardness of the workpiece before diamond burnishing process were observed to be 1.30-1.35 µm and 340 HV respectively.

Table 3. Results for surface roughness Ra (µm), and surface hardness H (HV).

Sl. No.	A	B	C	Ra (µm)	H (HV)
1	21	0.048	20	0.20	383
2	21	0.065	90	0.13	379
3	21	0.096	150	0.25	405
4	73	0.048	90	0.09	387
5	73	0.065	150	0.10	405
6	73	0.096	20	0.22	369
7	113	0.048	150	0.16	415
8	113	0.065	20	0.17	363
9	113	0.096	90	0.25	365

3. Results and discussion

The influence of diamond burnishing process parameters on the surface roughness and surface hardness can be obtained from the direct effect plot. Minitab 17.0 software has been used to obtain direct effect plot.

3.1. Effects of process parameters and cryogenic cooling on output responses

3.1.1. Surface roughness analysis

In any kind of machining process, surface roughness plays an important role. The main effect plot of surface roughness for the cryogenic environment is as depicted in Figure 3. In cryogenic diamond burnishing, as the burnishing speed increases from 21 m/min to 73 m/min the surface roughness decreases, and again it increases when the burnishing speed is increased to 113 m/min.

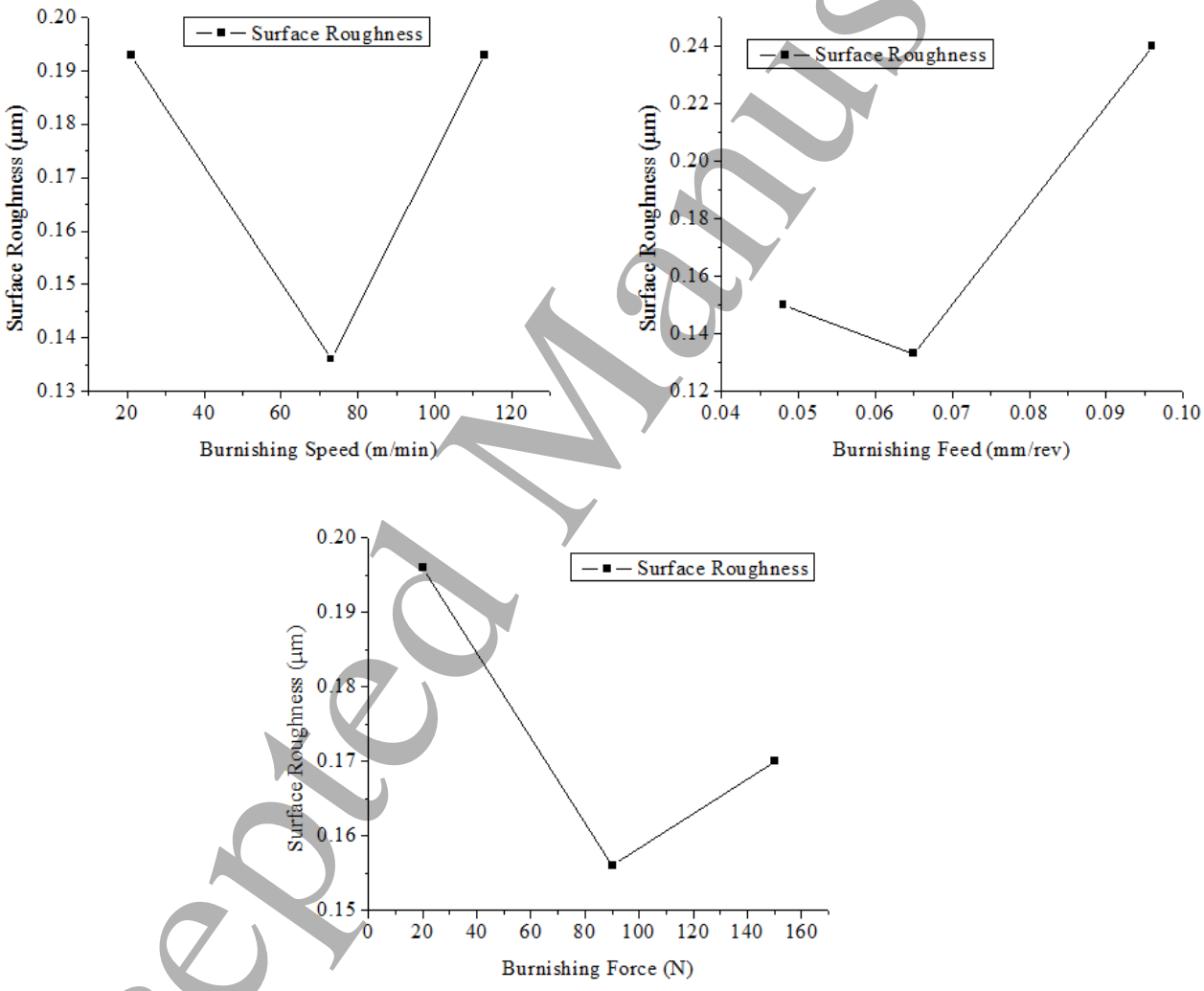

Figure 3. Direct effects plot of surface roughness for cryogenic burnishing

At lower burnishing speed, reduction in the surface roughness was observed because at this point the diamond tip will have more time to settle down the abnormalities and as the burnishing speed is gradually increased, temperature will increase at the tool-workpiece interface due to the

uneven movement of the tip along the workpiece surface, hence an increased surface roughness was observed [15]. As the burnishing feed increases from 0.048 mm/rev to 0.065 mm/rev, the surface roughness decreases and it increases with an increase in the burnishing feed. At lower burnishing feed, the distance between the successive traces of the tool tip is small, hence an improved surface finish can be observed. At higher burnishing feed, the distance between successive traces of the tool-tip will be high hence increased surface roughness can be observed [19]. Surface roughness decreases to a minimum value as the burnishing force increases from 20 to 90 N. Further increase in the burnishing force results in an increase in the surface roughness. It can be explained by the fact that as the burnishing force increases the plastic deformation will be high and which results in the formation of the deteriorated surface [17]. The minimum surface roughness of 0.09 µm was observed at burnishing speed of 73 m/min, burnishing feed of 0.048 mm/rev and burnishing force of 90 N. The simultaneous application of LN_2 reduces the temperature developed at the burnishing zone and it also results in lower friction generation which results in the improved surface finish.

3.1.2. Surface hardness analysis

The surface hardness was measured only on the top surface of the material which has been subjected to cryogenic diamond burnishing. The main effects plot of surface hardness for the cryogenic environment is depicted in Figure 4. In cryogenic diamond burnishing, as the burnishing speed increases from 21 m/min to 113 m/min, the surface hardness decreases. That's because, as the burnishing speed increases, the increase in the recovery of the work hardened surface takes place due to the increase in the temperature at the tool-workpiece interface [18]. In the Cryogenic environment, as the burnishing feed increases from 0.048 mm/rev to 0.096 mm/rev, the surface hardness decreases. It is because of the increase in the distances between the consecutive traces of the diamond tip [15]. As the burnishing force increases from 20 N to 150 N, the surface hardness increases. It is due to the improvement in the surface deformation taking place because of the increased burnishing force applied [16]. An improvement in surface hardness was observed at all the process parameters that's because, cooling the burnishing zone with the help of LN_2 leads to the formation of grain refinement that results in small grain formation which substantially increases the surface hardness of the material.

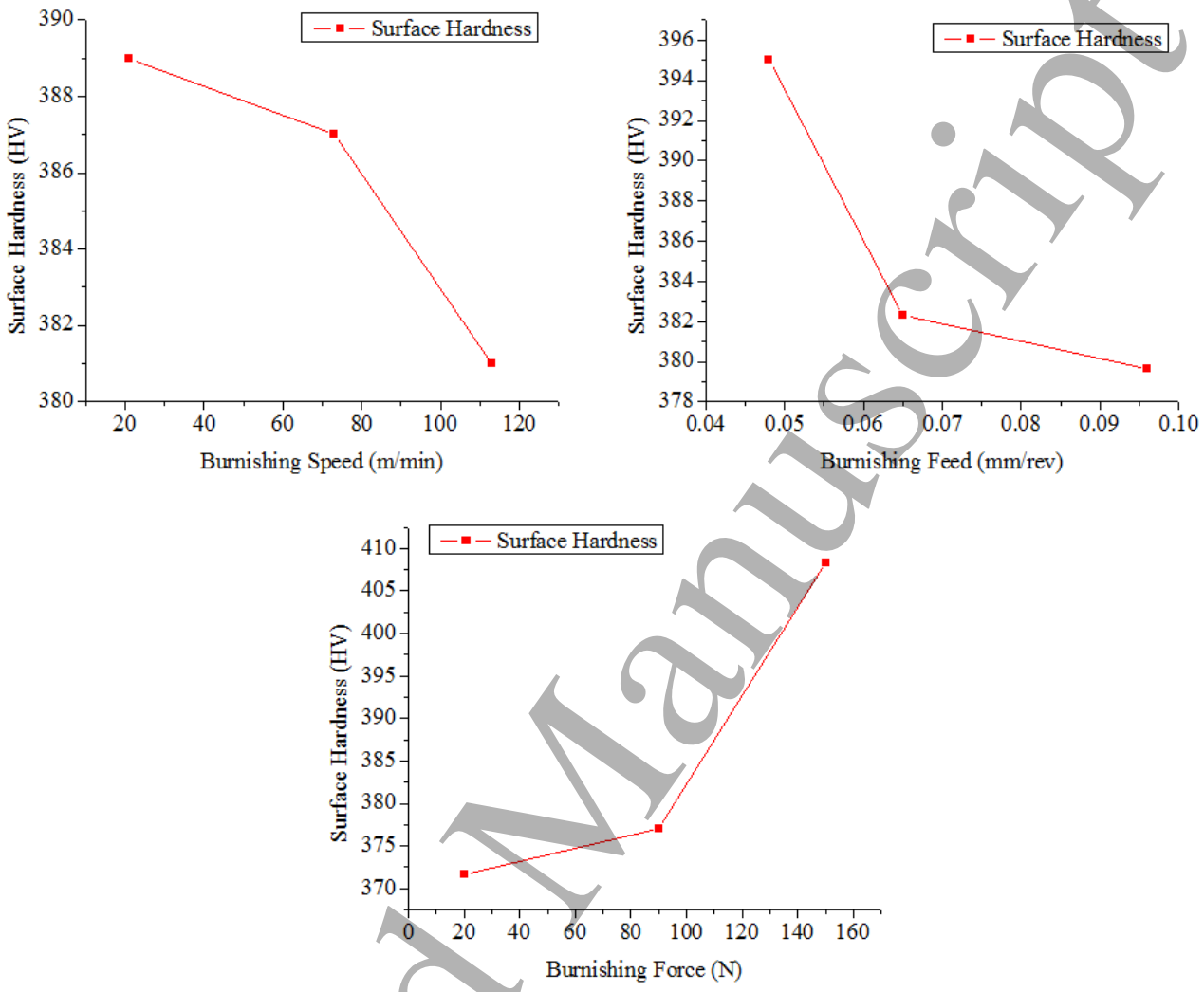

Figure 4. Direct effect plot of surface hardness for cryogenic burnishing

4. Grey relation-based Taguchi optimization

Grey relation system was proposed by Deng [19]. It is a tool which is used to analyze the process with multiple performance characteristics. Conversion of actual response values to those values which has been obtained by S/N ratios can be obtained by GRA. This method yields real data based results and also computations are easy to perform. The system which contains the information that is either incomplete or uncertain is called the grey relation system [13]. The multi-objective optimization problems are difficult to solve and with the effective implementation of GRA optimization of performance characteristics can be converted into single optimization with GRG. The experimental data obtained are normalized between the values 0-1. Many researchers

[20, 21, 22] have incorporated the following steps in Taguchi Grey relation analysis. Flowchart of the grey relation based Taguchi optimization is as described in Figure 5.

4.1. Preprocessing of data

Normalization is defined as a process of converting the original sequence into the comparable data sequence. The raw data from the different factors are normalized on a single scale of dimensions from multi-dimensions scales and are unified. The range of normalized values has to be performed in the range of zero to one. The normalization process is based on three categories: "the larger the better" for maximization objectives, "the nominal the better" for specific objective expectation and "the smaller the better" for minimization objective.

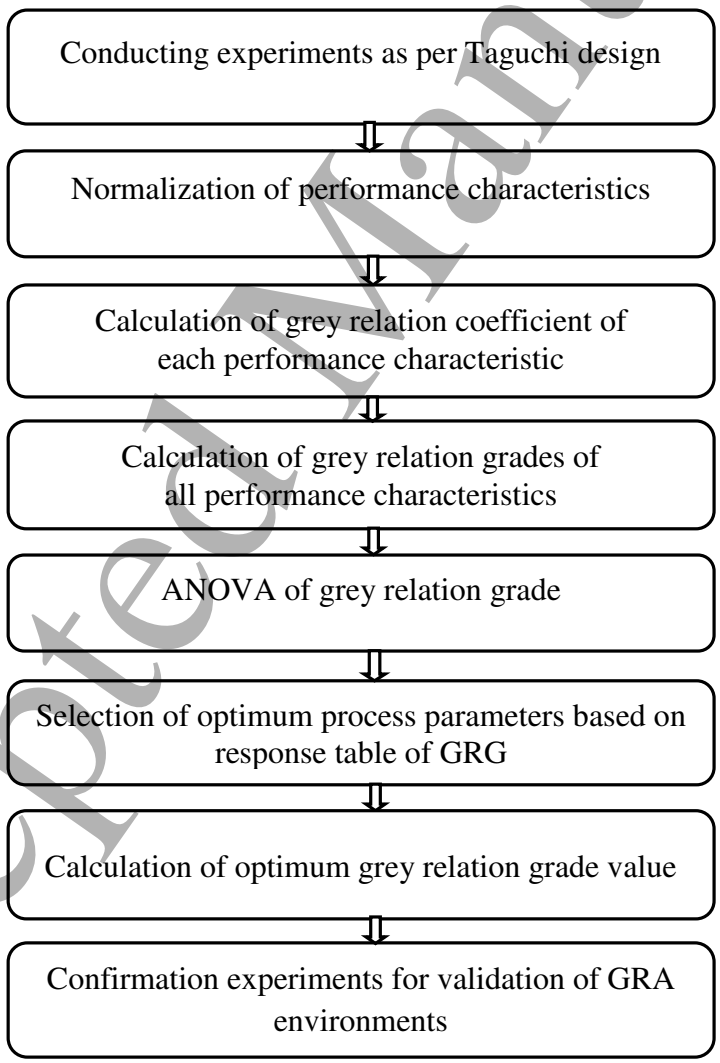

Figure 5. Methodology flow chart

In this research due to minimization and maximization of the objectives "the smaller the better" and "larger the better" normalization function is adapted for surface roughness and surface hardness respectively, which is defined in Eq.1 and Eq.2 respectively. The normalized data are depicted in Table 4.

$$D_i(r) = \frac{max\, E_i\,(r) - E_i\,(r)}{max\, E_i\,(r) - min E_i\,(r)} \quad (1)$$

$$D_i(r) = \frac{E_i\,(r) - min E_i\,(r)}{max\, E_i\,(r) - min E_i\,(r)} \quad (2)$$

Where, $E_i(r)$ is the original sequence, $D_i(r)$ is sequence after data preprocessing, max $E_i(r)$ and min $E_i(r)$ are the maximum and minimum values of the original data respectively.

Table 4. Preprocessing and deviation sequence

Trial No.	Preprocessing sequence		Deviation sequence	
	Ra	H	Ra	H
1	0.313	0.385	0.688	0.615
2	0.750	0.308	0.250	0.692
3	0.000	0.808	1.000	0.192
4	1.000	0.462	0.000	0.538
5	0.938	0.808	0.063	0.192
6	0.188	0.115	0.813	0.885
7	0.563	1.000	0.438	0.000
8	0.500	0.000	0.500	1.000
9	0.000	0.038	1.000	0.962

4.2. Grey relation coefficient

The relationship between the investigational and desirable results can be defined by calculating the grey relation coefficient. The grey relation coefficient can be computed by adapting Eq.3.

$$\varepsilon_i = \frac{\Delta_{min} + \zeta \Delta_{max}}{\Delta_{0i}(r) + \zeta \Delta_{max}} \quad (3)$$

Where $\Delta_{0i}(r)$ indicates absolute sequence deviation of sequence reference $D_0(r)$ and comparability sequence $D_i(r)$, i is the number of characteristics (1, 2, 3, 4) and r is the number of experimental runs (1, 2,……, 9). Hence $\Delta_{0i}(r)$ can be written as:

$$\Delta_{0i}(r) = \left| D_0(r) - D_i(r) \right| \quad (4)$$

$$\Delta_{min} = min_i\, min_r\, \Delta_{0i}(r) \quad (5)$$

$$\Delta_{max} = max_i\, max_r\, \Delta_{0i}(r) \quad (6)$$

The distinguishing co-efficient can have a value $\zeta \in [0, 1]$ and in this study $\zeta = 0.5$ has used to correct the difference of the relation co-efficient [23]. The computed difference sequence is listed in Table 4 and grey relation co-efficient in Table 5. Equation (4), (5) and (6) are used to calculate the values of Δ_{0i}, Δ_{min}, *and* Δ_{max}.

4.3. Grey relational grade (GRG)

Estimation of characteristics of multiple performances is performed by using GRG. The means of grey relation coefficient gives the GRG. Eq.7 is used to calculate GRG $\gamma_i(r)$ and obtained results along with GRG ranks are tabulated in Table 5.

$$\gamma_i(r) = \frac{1}{N}\sum_{i=0}^{n}[\omega_i * \varepsilon_i(r)] = \frac{1}{N}\sum_{i=0}^{n}\varepsilon_i(r) \qquad (7)$$

Where

N = is the no. of performance characteristics

ω_i = weights. In the present work, it is assumed that all control factors have equal importance.

Table 5. Grey relation coefficient and grades of grey relation

Trial No.	Grey relational co-efficient		Grey relational grade		
	Ra	H	Magnitude	S/N ratio	order
1	0.421	0.448	0.435	-7.230	6
2	0.667	0.419	0.543	-5.304	4
3	0.333	0.722	0.528	-5.547	5
4	1.000	0.481	0.741	-2.603	3
5	0.889	0.722	0.806	-1.873	1
6	0.381	0.361	0.371	-8.612	8
7	0.533	1.000	0.767	-2.304	2
8	0.500	0.333	0.417	-7.597	7
9	0.333	0.342	0.338	-9.421	9

Generally, the value should be in the range of 0 to1 ($0< \omega_i <1$). The larger GRG, the closer is the corresponding experimental responses to ideal values. It has been observed that multiple factors are transformed into single factors and preserved as a single-objective optimization problem. The "larger the better" approach is used in obtaining the signal-to-noise ratio for GRG. The signal-to-noise ratio values of GRG are tabularized in Table 5, and Minitab 17 software is used to compute the average for each level of control factors and the results are tabularized in Table 6. GRG results

of each parameter such as burnishing speed, burnishing feed, and burnishing force are depicted in Figure 6. From the analysis of means, $A_2B_1C_3$ is determined as the predicted optimal factors. The optimum factors are burnishing speed at 73 m/min, burnishing feed at 0.048 mm/rev and burnishing force of 150 N.

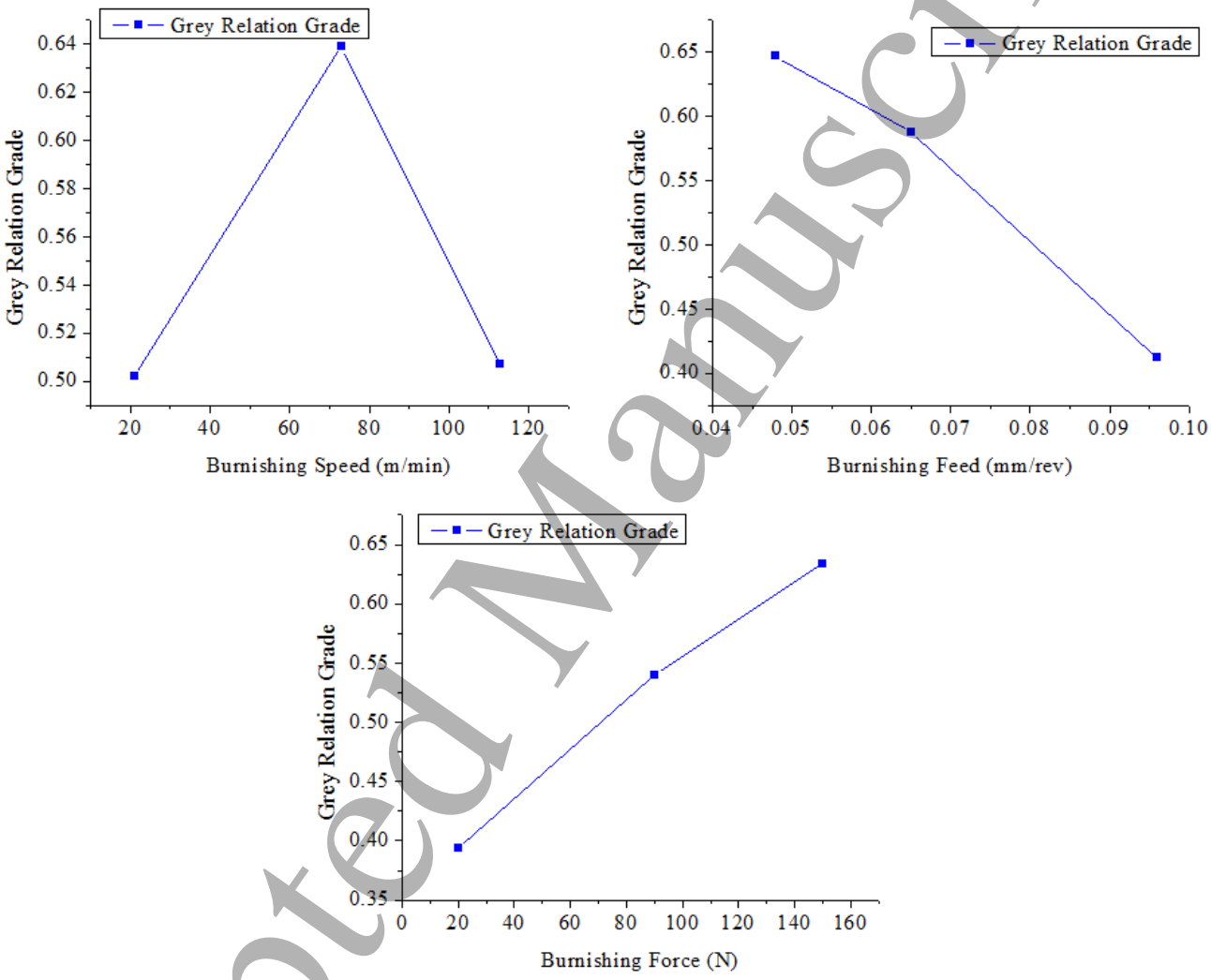

Figure 6. Main Effect plot for mean of means for GRG

Table 6. Response table for average GRG

Control factors	Level 1	Level 2	Level 3	Delta	Rank
A	0.5020	0.6393	0.5073	0.1373	3
B	0.6477	0.5887	0.4123	0.2353	2
C	0.3940	0.5407	0.6340	0.2400	1

4.4. Analysis of Variance (ANOVA)

To determine the effect of individual process parameters on diamond burnishing performance characteristics ANOVA has been performed for GRG data. From the Table 7, it is observed that burnishing feed has the highest contribution of 34.91% and is the most influenced parameter on diamond burnishing process. Burnishing feed is directly proportional to the surface roughness. Next most influencing process parameter is burnishing force with a contribution of 31.84% and the least possible contribution of 14.09% is observed in burnishing speed.

Table 7. ANOVA of grey relation grade

Factors	Degrees of freedom	Sum of square	Mean square	Factors Contribution (%)
A	2	0.0363	0.0368	14.09
B	2	0.0899	0.0250	34.91
C	2	0.0820	0.0410	31.84
Residual error	2	0.0492	0.0246	19.10
Total values	8	0.2575	-	-

4.5. Confirmation Experiments

To validate the perfection of performance characteristics while machining 17-4 PH stainless steel by using diamond burnishing tool confirmation assessment was performed. Optimum control factors selected for the confirmation test is as given in Table 8. The predictable GRG $\gamma_{predicted}$ using optimal conditions of the machining factors can be computed by using the Eq. 8.

$$\gamma_{predicted} = \gamma_m + \sum_{i=1}^{k}(\gamma_0 - \gamma_m) \qquad (8)$$

Where γ_m is the average of total grey relation grade, γ_0 is the means of GRG at their optimal levels, and k is the number of machining factors that considerably affects the multiple performance characteristics. The confirmation experimentations have been carried out at the optimal levels of performance measures. The GRG values of the confirmation test, initial and predicted are shown in Table 8. It was observed that the GRG attained at optimum cutting parameters combination is higher than that of the first experiment of Taguchi's L_9 orthogonal array.

Table 8. Response table for average grey relation grade

	Initial conditions	Optimal conditions	
		Prediction	Experimental
Level	$A_1B_1C_1$	$A_2B_1C_3$	$A_2B_1C_3$
Ra (μm)	0.20		0.17
H (HV)	383		412
Grey relation grade	0.4350	0.7886	0.7070
The improvement in grades of grey relation is 0.27			
The percentage improvement in GRG is 38.47			

5. Effect of process parameters and cryogenic cooling on surface morphology

Figure 7 (a) and (b) shows the SEM images of the diamond burnished surface which has been taken at two different conditions. In Figure 7(a), the surface defects such as micro cracks, and feed marks have been observed which may be due to the uneven flow of the material at that particular region. After obtaining the optimal condition based on GRA, the surface finish has been improved which can be seen from Figure 7 (b) and it can be observed that uniform surface has been obtained under the cryogenic environment at the optimal condition based on Taguchi grey system ($A_2B_1C_3$).

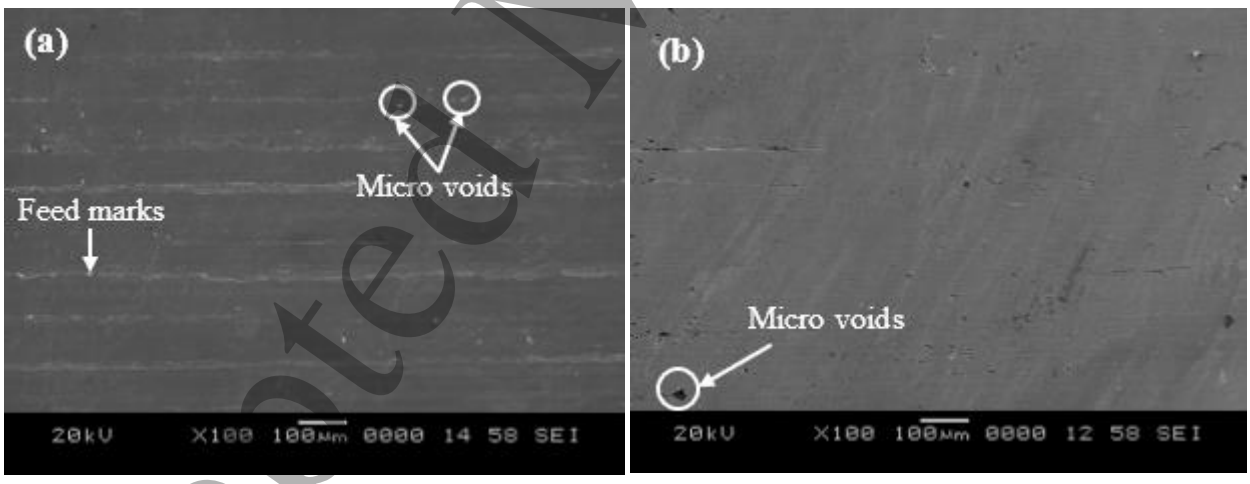

Figure 7. SEM images of the diamond burnished surface obtained under the cryogenic environment at (a) the orthogonal array No. 1 ($A_1B_1C_1$) condition (b) the optimal condition based on Taguchi grey system ($A_2B_1C_3$).

The surface defects have been minimized by the application of the LN_2 at the burnishing zone in both the conditions. It was observed that because of the diamond burnishing operation at the

cryogenic environment on the surface of the workpiece, led to the uniform flow of the metal which results in filling of most of the micro voids and hence uniform surface was obtained which results in reduced surface roughness. Figure 8(a) and (b) represents the 3D surface topography of the diamond burnished surface obtained at experiment number 1 and the optimal condition respectively. From the 3D surface topography, it can be seen that at the initial burnishing condition the surface roughness obtained was more because of the formation of high-intensity surface peaks which has been depicted in Figure 8(a). However, low peak to valley height has been observed under optimal diamond burnishing condition which is depicted in Figure 8(b). Hence the surface roughness has been reduced at the optimal diamond burnishing condition.

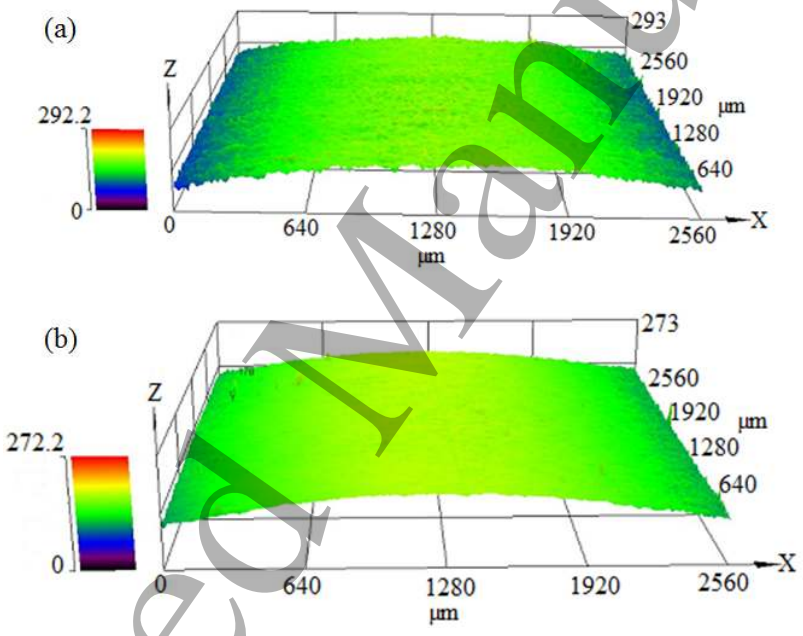

Figure 8. 3D surface topography of the diamond burnished surface obtained under the cryogenic environment at (a) the orthogonal array No. 1 ($A_1B_1C_1$) condition (b) the optimal condition based on Taguchi grey system ($A_2B_1C_3$).

6. Effect of process parameters and cryogenic cooling on microstructure of the specimen

The microstructure of the diamond burnished surface under cryogenic environment was obtained at orthogonal array No. 1 ($A_1B_1C_1$) condition and the optimal condition based on Taguchi grey system ($A_2B_1C_3$) is as depicted in Figure 9(a) and (b) respectively. It was observed that strong microstructural changes have been observed under both the conditions. A refined layer has been

formed after performing cryogenic diamond burnishing. The formation of a refined layer was because of the splashing of LN_2 at the tool-workpiece interface. The presence of the LN_2 initiates grain refinement at the top surface layer and the subsurface layer of the diamond burnished surface. The refinement of the grains is the major reason for the increased surface hardness and subsurface hardness of the specimen at different conditions which has been represented in Figure 4 and Figure 11 respectively. The refined layer thickness was measured for both the conditions. On an average, the refined layer thickness was measured to be 15 µm and 7 µm respectively for the optimal condition based on Taguchi grey system ($A_2B_1C_3$) and the orthogonal array No. 1 ($A_1B_1C_1$) condition respectively.

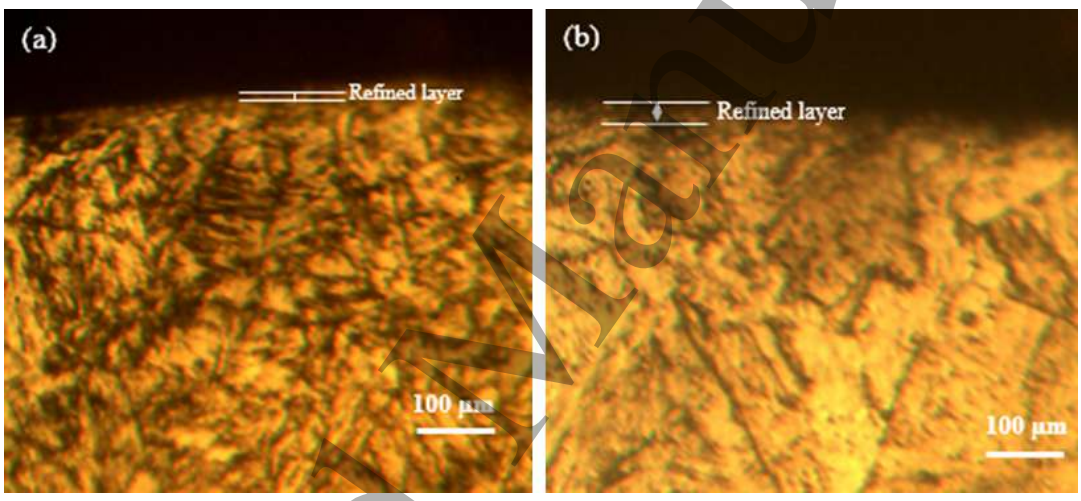

Figure 9. The microstructure of the diamond burnished subsurface obtained under the cryogenic environment at (a) the orthogonal array No. 1 ($A_1B_1C_1$) condition (b) the optimal condition based on Taguchi grey system ($A_2B_1C_3$)

7. Effect of process parameters and cryogenic cooling on subsurface hardness

The subsurface hardness measurement was performed for the sample which has been prepared as shown in Figure 10. The subsurface microhardness of the diamond burnished specimen was measured at orthogonal array No. 1 ($A_1B_1C_1$) condition and the optimal condition based on Taguchi grey system ($A_2B_1C_3$) is as represented in Figure 11.

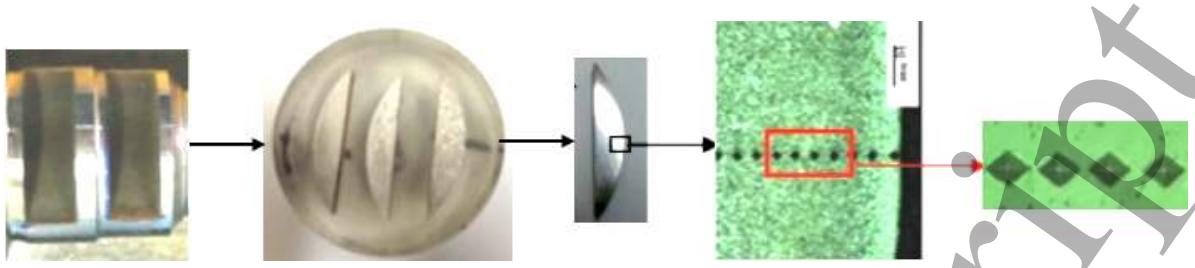

Figure 10. Subsurface microhardness measurement.

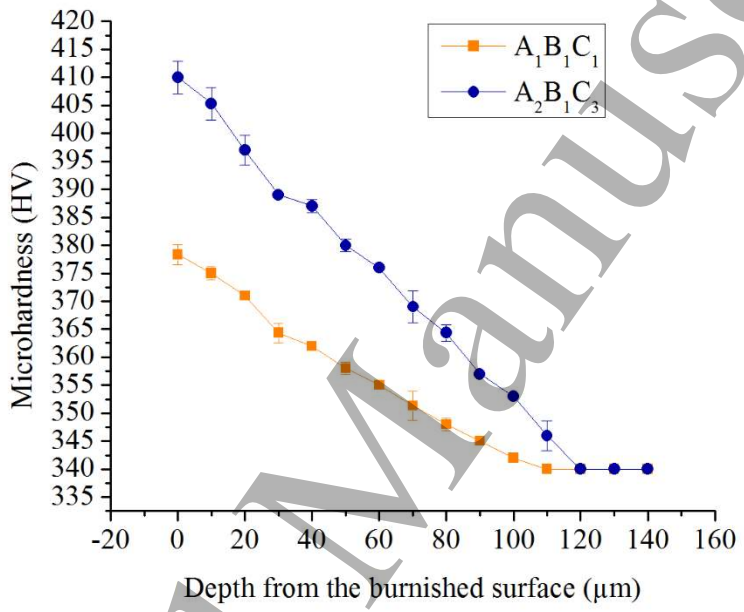

Figure 11. Subsurface microhardness of the diamond burnished surface obtained under the cryogenic environment at the orthogonal array No. 1 ($A_1B_1C_1$) and the optimal condition ($A_2B_1C_3$).

The subsurface microhardness was measured from the first point which is represented as 0 µm in Figure 11 indicates the depth just below the diamond burnished surface. The measurement have been taken up to a depth of 140 µm from the first point. That is only because, beyond this point, microhardness of the specimen reached the microhardness of the bulk material which is 340 HV. It was evident from the results of the subsurface microhardness that as the depth from the surface increases, the microhardness decreases and finally at some point it will reach the microhardness of the bulk material. This trend has been observed only because of the less shearing between the diamond tip and the sample surface and also due to the grain refinement taking place at the top surface layer of the specimen which could be observed in Figure 9. The splashing of the LN_2 has also been a major reason for the grain refinement which leads to increase in the

microhardness of the specimen. The maximum subsurface microhardness obtained at optimum condition and initial condition was 408 HV and 378 HV respectively. An improvement of 8% has been obtained at the optimal condition.

8. Conclusions

In this research, the diamond burnishing output responses, namely surface roughness, and surface hardness are optimized with respect to burnishing process conditions such as burnishing speed, burnishing feed and burnishing force at different levels. The 17-4 PH stainless steel was diamond burnished under the cryogenic environment. The following conclusions were drawn from the experimental results.

- From the multi-response optimization outcomes, the optimal process parameters are found to be burnishing speed 73 m/min, burnishing feed 0.048 mm/rev and burnishing force 150 N to minimize the surface roughness and maximize the surface hardness.
- The enhancement of GRG from primary parameter specifically $A_1B_1C_1$, to the optimum parameter combination $A_2B_1C_3$, was found to be 0.27. The improvement of GRG was observed to be 38.47%.
- Grain refinement has been observed in the microstructure of the specimen. A refined layer has been formed below the diamond burnished surface.
- Microhardness improvement of 8% has been achieved at the optimal diamond burnishing condition.

References

1. Mohanty, A., Gangopadhyay, S. and Thakur, A., 2016. On applicability of multilayer coated tool in dry machining of aerospace grade stainless steel. *Materials and Manufacturing Processes*, *31*(7), pp.869-879.
2. Wang, Z., Jiang, C., Gan, X., Chen, Y. and Ji, V., 2011. Influence of shot peening on the fatigue life of laser hardened 17-4PH steel. *International Journal of Fatigue*, *33*(4), pp.549-556.
3. Okada, M., Shinya, M., Matsubara, H., Kozuka, H., Tachiya, H., Asakawa, N. and Otsu, M., 2017. Development and characterization of diamond tip burnishing with a rotary tool. *Journal of Materials Processing Technology*, *244*, pp.106-115.
4. Patel, K.A. and Brahmbhatt, P.K., 2016. A comparative study of the RSM and ANN models for predicting surface roughness in roller burnishing. *Procedia Technology*, *23*, pp.391-397.
5. Yu, X. and Wang, L., 1999. Effect of various parameters on the surface roughness of an aluminium alloy burnished with a spherical surfaced polycrystalline diamond tool. *International Journal of Machine Tools and Manufacture*, *39*(3), pp.459-469.
6. Nestler, A. and Schubert, A., 2015. Effect of machining parameters on surface properties in slide diamond burnishing of aluminium matrix composites. *Materials Today: Proceedings*, *2*, pp.S156-S161.
7. Shaw, M. C. 1984, *Metal Cutting Principles*, Clarendon Press, Oxford Science Publication, UK.
8. Yang, S., Umbrello, D., Dillon, O.W., Puleo, D.A. and Jawahir, I.S., 2015. Cryogenic cooling effect on surface and subsurface microstructural modifications in burnishing of Co–Cr–Mo biomaterial. *Journal of Materials Processing Technology*, *217*, pp.211-221.
9. Caudill, J., Huang, B., Arvin, C., Schoop, J., Meyer, K. and Jawahir, I.S., 2014. Enhancing the surface integrity of Ti-6Al-4V alloy through cryogenic burnishing. *Procedia CIRP*, *13*, pp.243-248.
10. Aggarwal, A., Singh, H., Kumar, P. and Singh, M., 2008. Optimization of multiple quality characteristics for CNC turning under cryogenic cutting environment using desirability function. *Journal of Materials Processing Technology*, Vol. 205, No. 1, pp.42–50.

11. Tang, L. and Du, Y.T., 2014. Multi-objective optimization of green electrical discharge machining Ti–6Al–4V in tap water via Grey-Taguchi method. *Materials and Manufacturing Processes*, *29*(5), pp.507-513.
12. Chakradhar, D. and Gopal, A.V., 2011. Multi-objective optimization of electrochemical machining of EN31 steel by grey relational analysis. *International Journal of Modeling and optimization*, *1*(2), p.113.
13. Sivaiah, P. and Chakradhar, D., 2017. Multi-objective optimisation of cryogenic turning process using Taguchi-based grey relational analysis. *International Journal of Machining and Machinability of Materials*, *19*(4), pp.297-312.
14. Sivaiah, P. and Chakradhar, D., 2018. Multi performance characteristics optimization in cryogenic turning of 17-4 PH stainless steel using Taguchi coupled grey relational analysis. *Advances in Materials and Processing Technologies*, pp.1-17.
15. El-Taweel, T.A.; El-Axir, M.H., 2009. Analysis and optimization of the ball burnishing process through the Taguchi technique. *International Journal of Advanced Manufacturing Technology*, 41: pp.301–310.
16. El-Axir, M.H., Othman, O.M. and Abodiena, A.M., 2008. Study on the inner surface finishing of aluminum alloy 2014 by ball burnishing process. *journal of materials processing technology*, *202*(1-3), pp.435-442.
17. Nemat, M.; Lyons, A.C., 2000. An investigation of the surface topography of ball burnished mild steel and aluminium. *International Journal of Advanced Manufacturing Technology*, 16: pp.469–473.
18. Klocke, F., Bäcker, V., Wegner, H., Feldhaus, B., Baron, H.U. and Hessert, R., 2009. Influence of process and geometry parameters on the surface layer state after roller burnishing of IN718. *Production Engineering*, *3*(4-5), pp.391.
19. Deng, J., 1982. Control problems of grey systems. *Systems and Control Letters*, Vol. 1, No. 5, pp.288–294.
20. Sarıkaya, M. and Güllü, A., 2015. Multi-response optimization of minimum quantity lubrication parameters using Taguchi-based grey relational analysis in turning of difficult-to-cut alloy Haynes 25. *Journal of Cleaner Production*, *91*, pp.347-357.

21. Goel, B., Singh, S. and Sarepaka, R.V., 2015. Optimizing single point diamond turning for mono-crystalline germanium using grey relational analysis. *Materials and Manufacturing Processes*, *30*(8), pp.1018-1025.
22. Senthilkumar, N., Tamizharasan, T. and Anandakrishnan, V., 2014. Experimental investigation and performance analysis of cemented carbide inserts of different geometries using Taguchi based grey relational analysis. *Measurement*, *58*, pp.520-536.
23. Mia, M., Khan, M.A., Rahman, S.S. and Dhar, N.R., 2017. Mono-objective and multi-objective optimization of performance parameters in high pressure coolant assisted turning of Ti-6Al-4V. *The International Journal of Advanced Manufacturing Technology*, *90*(1-4), pp.109-118.